

Synthesis and Characterization of Phenylnitroxide-Substituted Zinc(II) Porphyrins

David A. Shultz,* Kevin P. Gwaltney, and Hyoyoung Lee

Department of Chemistry, North Carolina State University, Raleigh, North Carolina 27695-8204

Received September 16, 1997

The syntheses and fluid-solution EPR spectra of nitroxide-substituted porphyrins **1–3** are described. The phenylnitroxide is attached to the *meso*-position of three porphyrins: (a) directly through a single bond (**1**); (b) through an ethenyl group (**2**); and (c) through an ethynyl group (**3**). The spin distribution in each of the three radicals is discussed and compared to model compounds **4–9**. It is suggested that delocalization increases in the order **2, 1, 3**.

We are preparing radical-substituted metalloporphyrins for construction of coordination polymers with interesting magnetic properties.^{1,2} There are several design motifs for such materials, including coupling the organic radical spin with the unpaired electron of an oxidized porphyrin, coupling with a transition metal spin, or coupling with both. Conjugation of a radical with the porphyrin ring (and therefore coupling with any paramagnetic metal bound therein) will occur provided that the torsion angle between the radical and the porphyrin is not 90°. To avoid a severe torsion angle,³ a *meso*-aryl ring can be separated from the porphyrin ring by, for example, an ethenyl or an ethynyl group.⁴

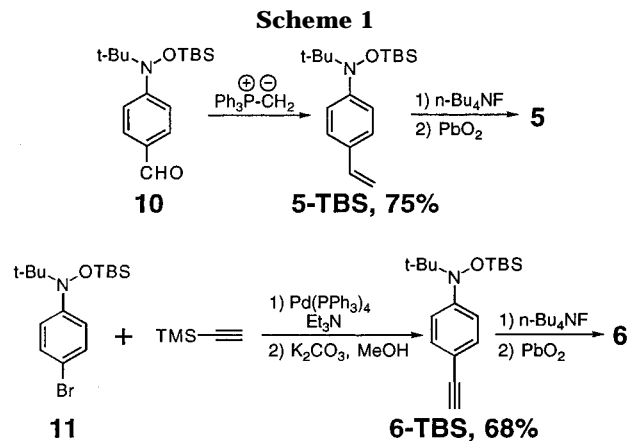
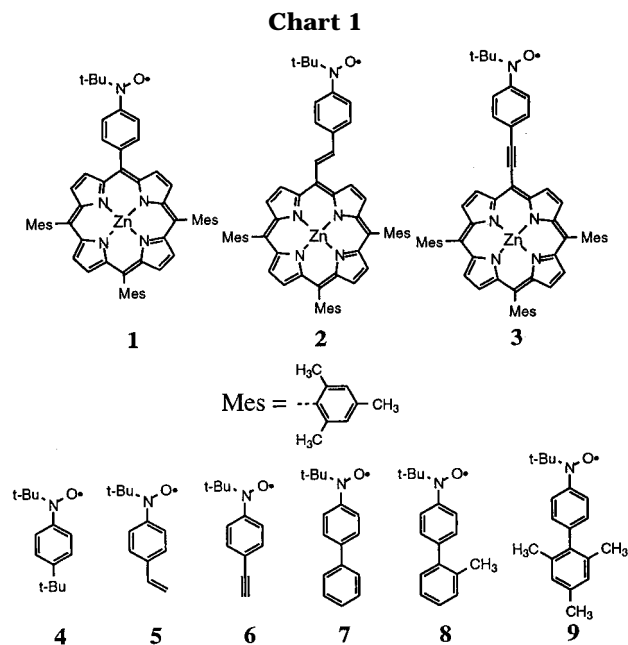
In such cases, the conjugative effectiveness of the fragment that links the porphyrin and the aryl group is critical for sufficient spin–spin communication. Herein, we describe the preparation and EPR spectral properties of Zn(II) porphyrins **1–3**, which will be used to examine linker effectiveness and other structure–property relationships. Porphyrins **1–3** each have one phenylnitroxide bound to a *meso*-position: directly (**1**); through a carbon–carbon double bond (**2**); and through a carbon–carbon triple bond (**3**). We chose to occupy the remaining *meso*-positions with mesityl groups, which will not affect nitroxide conjugation since mesityl torsion angles are nearly 90°. The fluid solution EPR spectra of **1–3** are compared to model compounds **4–9** (Chart 1).

(1) Shultz, D. A.; Knox, D. A.; Morgan, L. W.; Sandberg, K.; Tew, G. N. *Tetrahedron Lett.* **1993**, *34*, 3975.

(2) For studies of porphyrinic magnetic materials, see the following: (a) Conklin, B. J.; Sellers, S. P.; Fitzgerald, J. P.; Yee, G. T. *Adv. Mater.* **1994**, *6*, 836. (b) Kamachi, M.; Cheng, X.; Aota, H.; Mori, W.; Kishita, M. *Chem. Lett.* **1987**, 2331. (c) Kitano, M.; Koga, N.; Iwamura, H. *J. Chem. Soc., Chem. Commun.* **1994**, 447. (d) Kitano, M.; Ishimaru, Y.; Inoue, K.; Koga, N.; Iwamura, H. *Inorg. Chem.* **1994**, *33*, 6012. (e) Koga, N.; Iwamura, H. *Nihon Kagaku Naishi* **1989**, 1456. (f) Miller, J. S.; Vazquez, C.; Epstein, A. J. *J. Mater. Chem.* **1995**, *5*, 707. (g) Miller, J. S.; Bohm, A.; Vazquez, C. *Inorg. Chem.* **1996**, *35*, 3083. (h) Miller, J. S.; Calabrese, J. C.; McLean, R. S.; Epstein, A. J. *Adv. Mater.* **1992**, *4*, 498.

(3) Typically, *meso*-aryl groups are twisted 60–90°. Scheidt, W. R.; Lee, Y. J. In *Structure and Bonding*, Vol. 64; Buchler, J. W., Ed.; Springer-Verlag: Berlin, 1987; pp 1–70.

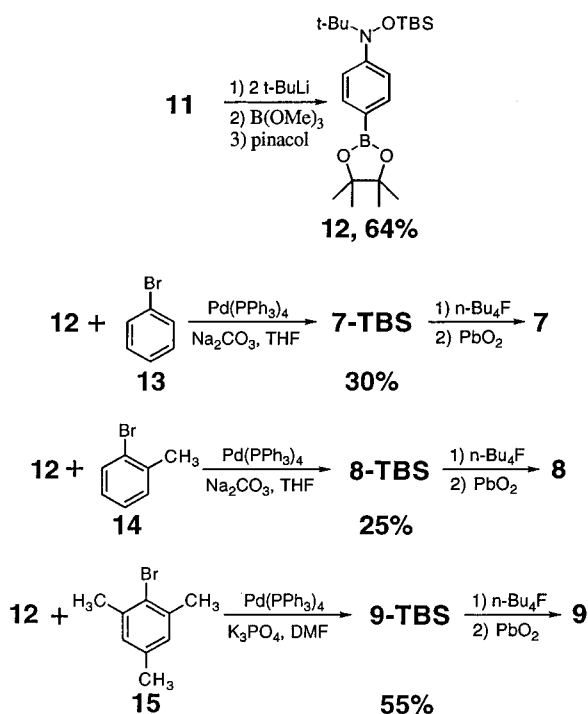
(4) For *meso*-alkenyl- and -alkynylporphyrin syntheses, see the following: (a) Boyle, R. W.; Johnson, C. K.; Dolphin, D. *J. Chem. Soc., Chem. Commun.* **1995**, 527. (b) Higuchi, H.; Shimizu, K.; Ojima, J. *Tetrahedron Lett.* **1995**, *36*, 5359. (c) LeCours, S. M.; Guan, H.-W.; DiMaggio, S. G.; Wang, C. H.; Therien, M. J. *J. Am. Chem. Soc.* **1996**, *118*, 1497. (d) Milgrom, L. R.; Yahioğlu, G. *Tetrahedron Lett.* **1996**, *37*, 4069. (e) Yashunsky, D. V.; Ponomarev, G. V. *Tetrahedron Lett.* **1995**, *36*, 8485. (f) Jiang, X.; Nurco, D. J.; Smith, K. M. *Chem. Commun.* **1996**, 1759. (g) Arnold, D. P.; James, D. A. *J. Org. Chem.* **1997**, *62*, 3460. (h) Anderson, H. L. *Tetrahedron Lett.* **1992**, *33*, 1101.



Model compound **4** was prepared according to a modified version of the published procedure,⁵ while **5-TBS** was prepared from the (4-formylphenyl)-TBS-nitroxide **10** using the Wittig reaction, as shown in Scheme 1. Acetylene **6-TBS** was prepared from Pd-catalyzed coupling of

(5) Calder, A.; Forrester, A. R. *J. Chem. Soc., Chem. Commun.* **1967**, 682.

Scheme 2



TMS-acetylene and (4-bromophenyl)-TBS-nitroxide **11**,⁶ followed by removal of the TMS group. Radicals **4–6** were generated by fluoride deprotection of the TBS ethers followed by PbO_2 oxidation.

Nitroxide radicals **7⁵–9** were prepared as shown in Scheme 2. Boronic ester **12** was synthesized by transmetalation of **11**, reaction with trimethylborate, and subsequent condensation with pinacol.⁷ Suzuki coupling⁸ of **12** and commercially available bromides **13–15** provided the TBS ethers. Radical formation was accomplished as described for **4–6**.

The syntheses of nitroxide porphyrins **1–3**, shown in Scheme 3, feature Pd-catalyzed coupling reactions of 5-iodo-10,15,20-trimesitylporphyrin with the appropriate TBS-protected phenylnitroxide boronate,⁸ alkene,⁹ and alkyne.¹⁰ Fluoride-promoted TBS deprotection and PbO_2 oxidation provided nitroxide porphyrins **1–3**. 5-Iodo-10,15,20-trimesitylporphyrin was prepared by reacting dipyrromethane,¹¹ mesityldipyrromethane¹² with 2 equiv of mesitaldehyde according to the method of Lindsey¹² and subsequently iodinating according to a modified procedure of Dolphin.^{13,14}

The spin distributions in **1–9** can be evaluated by comparing the hyperfine coupling constants (hfcc), since

(6) Inoue, K.; Iwamura, H. *Angew. Chem., Int. Ed. Engl.* **1995**, *34*, 927.

(7) Lamba, J. J. S.; James, M.; Tour, J. M. *J. Am. Chem. Soc.* **1994**, *116*, 11723.

(8) Miyaura, N.; Yanagi, T.; Suzuki, A. *Synth. Commun.* **1981**, *11*, 513.

(9) The Heck conditions used were those reported by Yu: Bao, Z.; Chen, Y.; Cai, R.; Yu, L. *Macromolecules* **1993**, *26*, 5281.

(10) LeCours, S. M.; Guan, H.-W.; DiMugno, S. G.; Wang, C. H.; Therien, M. J. *J. Am. Chem. Soc.* **1996**, *118*, 1497.

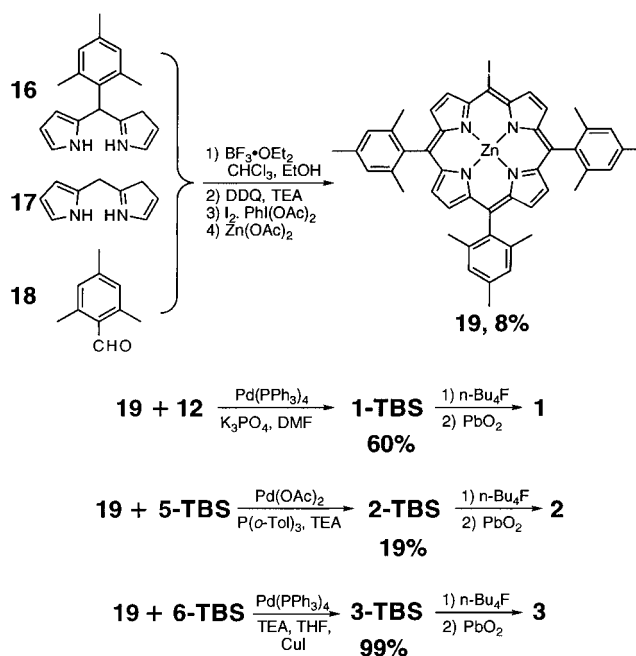
(11) Wang, Q. M.; Bruce, D. W. *Synlett* **1995**, 1267.

(12) Lee, C.-H.; Lindsey, J. S. *Tetrahedron* **1994**, *50*, 11427.

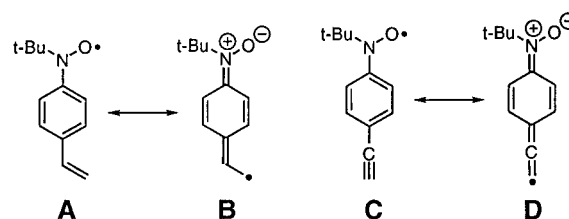
(13) Boyle, R. W.; Johnson, C. K.; Dolphin, D. *J. Chem. Soc., Chem. Commun.* **1995**, 527.

(14) We found that using 0.5 equiv of bis(acetoxy)phenyl iodide: iodine resulted in better yields of product, according to the procedure of Merkushev: Merkushev, E. B.; Simakhina, N. D.; Koveshnikova, G. M. *Synthesis* **1980**, 486.

Scheme 3



the latter are directly proportional to spin densities.^{15–19} We reasoned that torsion of the phenyl ring bearing the nitroxide group in **1** would dramatically diminish interaction with the porphyrin, and C=C should be more effective than C≡C for spin delocalization. Therefore, interaction of the nitroxide with the porphyrin might increase from **1** to **3** to **2**. However, steric interactions between β -pyrrole hydrogens and C=C hydrogens in **2** (as with phenyl hydrogens in **1**) that are absent in **3** could alter the proposed ordering. Our reasoning that C=C should be more effective than C≡C for spin delocalization in the absence of torsion is based on the resonance structures **A–D**. Conjugation through C≡C results in a cumulenonic resonance form, **D**, which is less favorable than the corresponding noncumulenonic form, **B**.



The fluid solution EPR spectra of **1–6**, and spectral simulations²⁰ are shown in Figure 1, while EPR spectra of model compounds **7–9** and simulations²⁰ are shown in Figure 2. Proton and nitrogen hfcc for **1–9** obtained from the simulations are listed in Table 1. Unfortunately, no hfcc due to porphyrinic nuclei were observed. Experimental spectra for **1–3** exhibit asymmetric line

(15) Weissman, S. I. *J. Chem. Phys.* **1956**, *25*, 890.

(16) McConnell, H. M. *J. Chem. Phys.* **1956**, *24*, 764.

(17) McConnell, H. M.; Chestnut, D. B. *J. Chem. Phys.* **1958**, *28*, 107.

(18) Bersohn, R. *J. Chem. Phys.* **1956**, *24*, 1066.

(19) Wertz, J. E.; Bolton, J. R. *Electron Spin Resonance*; Chapman and Hall: New York, 1986.

(20) Fluid solution EPR spectra were simulated using the following: Duling, D. EPR Calculations for MS-Windows NT/95, Version 0.96, Public EPR Software Tools, National Institute of Environmental Health Sciences, National Institutes of Health, Research Triangle Park, NC, 1996.

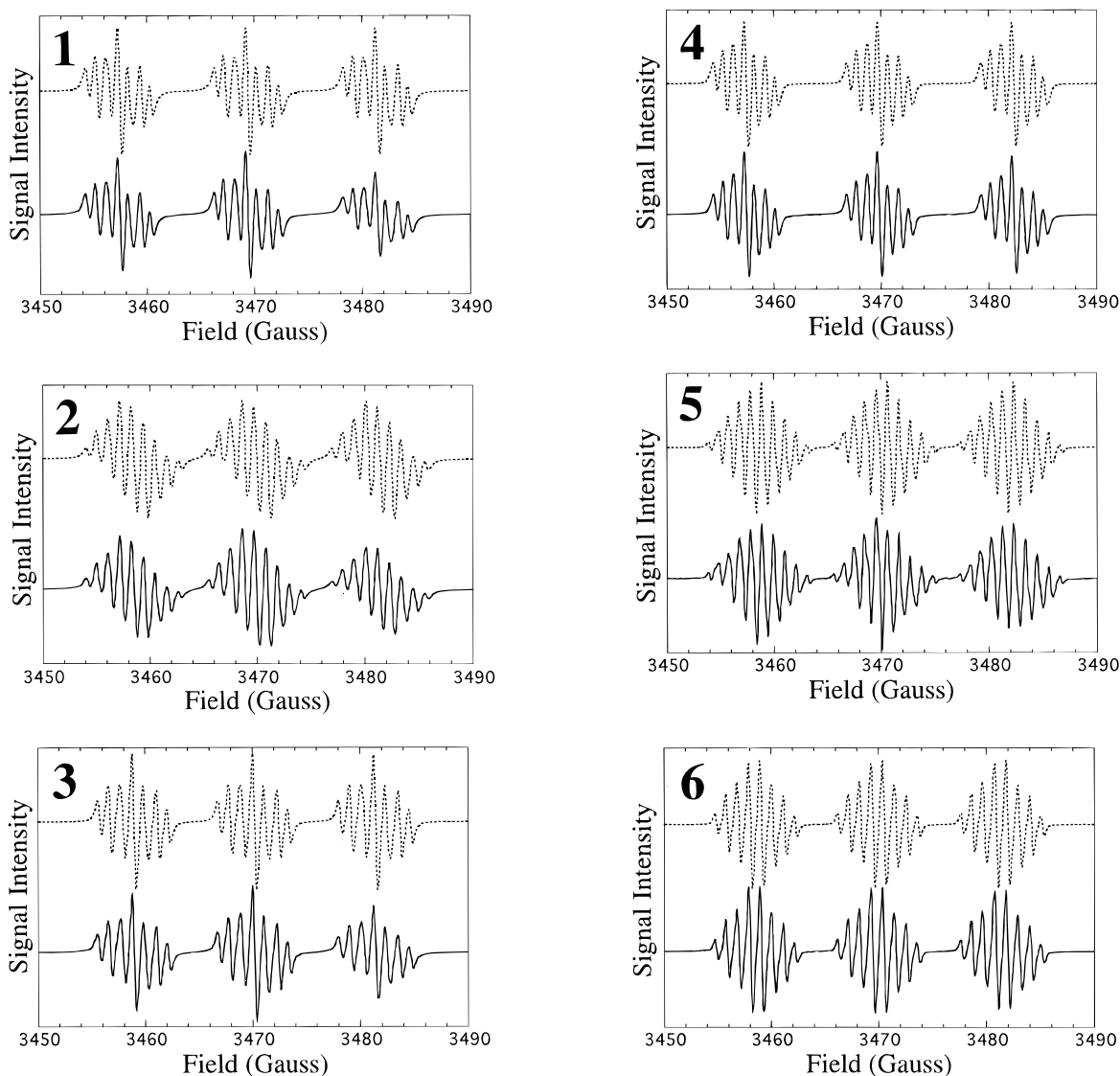


Figure 1. X-band EPR spectra of porphyrins **1–3** (left) and model compounds **4–6** (right) in toluene recorded at 298 K. Each plot includes a simulated spectrum, top (---), and an experimental spectrum, bottom (—). Best fit simulations were achieved using hfcc listed in Table 1. The simulations were accomplished using a Simplex fitting routine, and all correlation coefficients exceeded 0.98.²⁰

broadening presumably due to either slow tumbling of the large porphyrin molecules or anisotropic diffusion.²¹ Thus, the high-field lines are broadened relative to the low-field lines, which in turn are broader than the central lines, as is observed for viscous solutions of di-*tert*-butylnitroxide.¹⁹

The hfcc values in Table 1 show that the a_N decreases and the ring- a_H increases from **1–3**, and from **4–6**, consistent with increased conjugation in the same order—contrary to our prediction based on resonance structures **A–D**. However, this trend is expected on the basis of the known correlation of aryl nitroxide a_N with the substituent parameter, σ_p :^{22–26} -0.04 for $\text{CH}=\text{CH}_2$ and $+0.23$ for $\text{C}\equiv\text{CH}$.²⁷ The more electron-withdrawing

$\text{C}\equiv\text{C}$ draws more spin density into the phenyl ring away from the nitrogen than does $\text{C}=\text{C}$, not necessarily because of increased conjugation, but because the electronegativity of an sp -hybridized carbon is greater than an sp^2 -hybridized carbon. Moreover, comparison of the $=\text{CH}_2$ H-hfcc of **5** ($a_H = 1.01$ G) to the H-hfcc of the $\equiv\text{CH}$ proton of **6** ($a_H = 0.95$ G) shows that slightly more spin density reaches $\text{C}=\text{C}$ than reaches $\text{C}\equiv\text{C}$; thus $\text{C}\equiv\text{C}$ is better than $\text{C}=\text{C}$ at withdrawing spin into the phenyl ring, but not quite as effective at further delocalization. It appears that the supposed intrinsic difference in ability to conjugate between $\text{C}=\text{C}$ and $\text{C}\equiv\text{C}$ is attenuated, and in this case the two groups are nearly equal in their ability to conjugate.

Examination of the phenyl ring H-hfcc and N-hfcc of **2** compared to **5** and **3** compared to **6** show that additional spin density is delocalized away from the nitrogens in porphyrins **2** and **3**. Whether this additional spin density

(21) Hudson, A.; Luckhurst, G. R. *Chem. Rev.* **1969**, *69*, 191.

(22) Strom, E. T.; Bluhm, A. L.; Weinstein, J. *J. Org. Chem.* **1967**, *32*, 3853.

(23) Church, D. F. *J. Org. Chem.* **1986**, *51*, 1138.

(24) Lemaire, H.; Marechal, Y.; Ramasseul, R.; Rassat, A. *Bull. Soc. Chim. Fr.* **1965**, 372.

(25) Neugebauer, F. A.; Fischer, P. H. H. *Z. Naturforsch* **1966**, *21b*, 1036.

(26) Zhang, Y. H.; Jiang, B.; Zhou, C. M.; Jiang, X. K. *Chin. J. Chem.* **1994**, *12*, 516.

(27) Hansch, C.; Leo, A.; Taft, R. W. *Chem. Rev.* **1991**, *91*, 165.

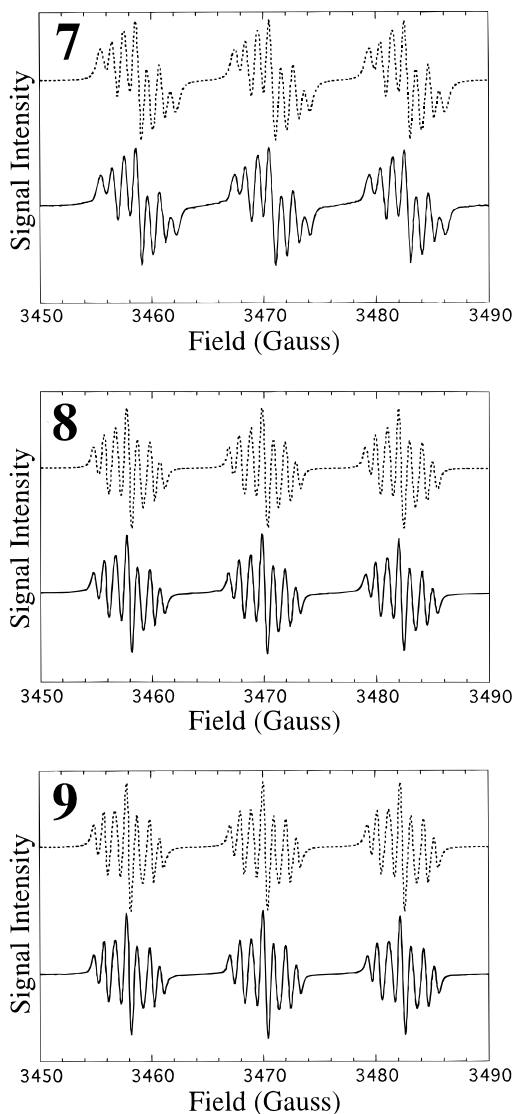


Figure 2. X-band EPR spectra of toluene solutions of model compounds 7–9 recorded at 298 K. Each plot includes a simulated spectrum, top (---), and an experimental spectrum, bottom (—). Best fit simulations were achieved using hfcc listed in Table 1. The simulations were accomplished using a Simplex fitting routine, and all correlation coefficients exceeded 0.98.²⁰

Table 1. EPR ¹⁴N- and ¹H-Hyperfine Coupling Constants for 1–9^a

compd	<i>a</i> _N /G	<i>a</i> _{o-H} /G	<i>a</i> _{m-H} /G	<i>a</i> _H /G ^b	line width/G
1	11.99	2.08	0.87		0.36
2	11.44	2.16	0.94	0.99, 1.31	0.38
3	11.23	2.24	0.99		0.32
4	12.46	1.97	0.87		0.33
5	11.72	2.17	1.01	0.77, 1.01 ^c	0.23
6	11.43	2.19	1.04	0.95	0.21
7	11.94	2.12	0.93		0.46
8	12.10	2.03	0.88		0.31
9	12.18	2.03	0.88		0.31

^a 0.1 mM toluene solutions at 298 K; hfcc (± 0.01 G) and line widths from spectral simulations.²⁰ ^b Ethenyl, ethynyl, or aryl H. ^c Terminal H.

is due to a change in electron demand of the substituents (ethenyl vs. 2-porphyrinylethenyl and ethynyl vs. 2-porphyrinylethynyl) or due to extended conjugation awaits further studies.

What about porphyrin **1**, in which the phenyl nitroxide is directly bound to the porphyrin *meso*-position? Is

compound **4** an appropriate model compound? Probably not. Regardless of the torsion angle between the phenyl and porphyrin rings, the carbon attached to the phenyl ring in **1** is sp² hybridized while the carbon bound to the phenyl ring in **4** is sp³ hybridized, and therefore, *a*_N(**4**) is greater than *a*_N(**1**), consistent with the cited substituent effect (*σ*_p(*t*-Bu) = −0.20).²⁷ Perhaps compounds 7–9 are better models of **1** since the aryl rings in 7–9 all have sp² carbons attached to the phenyl ring of the nitroxide. However, comparing **1** to 7–9 ignores differences in electron demand between phenyl and porphyrinyl. Unfortunately, to our knowledge there is no *σ*_p for porphyrinyl.

MM2 calculations^{28,29} on biphenyl, 2-methylbiphenyl, and 2,4,6-trimethylbiphenyl give phenyl–aryl torsion angles of 45°, 54°, and 62°, respectively. It is evident that the *a*_N values decrease as torsion increases. In fact, the calculated torsion for **9** is quite close to measured phenyl torsions in tetraphenylporphyrins.³ Nevertheless, *a*_N(**1**) is closest to *a*_N(**7**), suggesting similar delocalization in **1** and **7**. However, comparison of the spectrum of **7** with that of **1** indicates that additional hf-induced line broadening is absent in **1**, and therefore, conjugation in **1** is less than that in **7**. Since the spin density delocalized into the phenyl substituent of **7** is small, and this small spin density is spread over several atoms, the substituent-hfcc are quite small and are manifested only in the line width. We believe therefore that delocalization in **1** is closest to that in **9** and that the differences in *a*_N between **1** and **9** are because of the differences in electronegativity between porphyrin and phenyl.

Because of the lack of porphyrin-hfcc and the absence of a “linker” in **1**, our hfcc analysis does not permit us to distinguish with absolute certainty delocalization in **1** vs. **2** or **3**. Moreover, we cannot ascertain whether porphyrin rings have identical geometries in 1–3 and how porphyrin ring geometry might affect spin delocalization. Nevertheless, we propose the following: (a) phenyl torsion in **1** is substantial³ and we surmise that ethenyl torsion in **2** is similarly large, such that delocalization in **2** is less than in **1**; (b) since the ethenyl and ethynyl fragments are nearly equivalent at attracting spin density to the carbon attached to the porphyrin, and ethenyl is twisted relative to the porphyrin ring, **3** will be more delocalized than **2**; (c) since **3** can achieve planarity, delocalization will be greater than in **1**. Proposition (a) is sensible since there is less spin density at the ethenyl carbon attached to the porphyrin *meso*-position in **2** than spin density at the *para*-carbon attached to the porphyrin *meso*-position in **1**. Thus, we propose that delocalization increases in the order **2** < **1** < **3**.

In summary, we prepared three new zinc porphyrins bearing nitroxide radicals that are conjugated with the porphyrin ring. The factors that affect spin delocalization were examined, and a relative ordering of interaction of the radical with the porphyrin ring was suggested. It appears that C=C is only a slightly better conjugating group than C≡C for nitroxide radicals. As an addition to the known substituent effect on *a*_N, we showed that increased torsion measurably alters *a*_N. The limitations of using hfcc for determining spin distributions in nitroxide radicals were pointed out. Further studies of spin delocalization in molecules 1–3 are underway.

(28) Allinger, N. L. *J. Am. Chem. Soc.* **1977**, *99*, 8127.

(29) Allinger, N. L.; Yuh, Y. H. *QCPE* **1981**, *13*, 395.

Experimental Section

Solvent distillations, synthetic procedures, and EPR sample preparation were carried out under an argon or nitrogen atmosphere. THF and toluene were distilled from sodium benzophenone–ketyl prior to use. Chloroform for porphyrin synthesis was distilled from K_2CO_3 . Anhydrous DMF was purchased from Aldrich. Boron trifluoride etherate was purchased from Lancaster. NMR spectra were recorded on a Varian 300 MHz spectrometer using either deuteriochloroform as solvent and referenced to protiochloroform at 7.26 ppm for 1H spectra and 77.0 ppm for ^{13}C spectra or deuteriomethylene chloride as solvent and referenced to protiomethylene chloride at 5.32 ppm for 1H spectra and 54.0 ppm for ^{13}C spectra. Elemental analysis was performed by Atlantic Microlab, Inc. Norcross, GA. X-band EPR spectra were recorded on an IBM-Brüker E200SRC spectrometer. Compound **4** was prepared as described in ref 5, except that the aryllithium was used instead of the Grignard.

Zinc(II) 5-[4-[*N*-*tert*-butyl-*N*-(*tert*-butyldimethylsiloxy)-amino]phenyl]-10,15,20-trimesitylporphyrin (1-TBS). A 25 mL flask containing compound **19** (70 mg, 0.082 mmol), $Pd(PPh_3)_4$ (4.7 mg, 4.1 μ mol), and compound **12** (44.1 mg, 0.123 mmol) in anhydrous DMF (4 mL) was stirred while sparging with argon for 10 min. K_3PO_4 (0.1778 g, 0.123 mmol) was added quickly with argon purging and heated for 7 h. Once cool, the solvent was removed by vacuum transfer. The mixture was dissolved in petroleum ether and filtered through silica. The solvent was removed under reduced pressure. The residue was purified by radial chromatography (1% ether–pentane) to give a pink solid, **1-TBS** (0.049 g, 60%): 1H NMR ($CDCl_3$) δ 8.89 (d, 2H, $J = 4.5$ Hz), 8.74 (d, 2H, $J = 4.6$ Hz), 8.70 (s, 4H), 8.09 (d, 2H, $J = 8.1$ Hz), 7.65 (d, 2H, $J = 8.0$ Hz), 7.29 (bs, 6H), 2.62 (s, 9H), 1.85 (s, 6H), 1.84 (s, 12H), 1.38 (s, 9H), 1.05 (s, 9H), -0.17 (bs, 6H); ^{13}C NMR ($CDCl_3$) δ 151.2, 150.7, 150.4, 150.4, 139.8, 139.8, 139.7, 139.6, 138.1, 134.0, 132.7, 131.6, 131.5, 130.9, 128.2, 124.1, 120.9, 119.3, 119.1, 61.6, 26.8, 26.6, 22.0, 21.9, 21.8, 18.6, -4.2 ; UV–Vis ($CHCl_3$) λ_{max} (log ϵ) 594 (3.33), 553 (4.06), 509 (3.39), 482 (3.42), 423 (5.39), 403 (4.37), 309 (4.08). IR (film) ν_{max} 3116, 2958, 2927, 2857, 1610, 1525, 1496, 1480, 1458 cm^{-1} ; MS–FAB $C_{63}H_{69}N_5O-SiZn$ calcd exact mass 1003.4563, obsd 1003.4571. Anal. Calcd for $C_{63}H_{69}N_5O-SiZn$: C, 75.23; H, 6.91. Found: C, 75.38; H, 7.00.

Zinc(II) 5-[4-[*N*-*tert*-butyl-*N*-(*tert*-butyldimethylsiloxy)-amino]phenylethynyl]-10,15,20-trimesitylporphyrin (2-TBS). In a 25 mL round-bottom flask fitted with a condenser were heated **19** (100 mg, 0.117 mmol), **5-TBS** (44 mg, 0.144 mmol), $Pd(OAc)_2$ (2.3 mg, 0.010 mmol), tri-*o*-tolylphosphine (11.9 mg, 0.039 mmol), triethylamine (29.6 mg, 0.293 mmol) and DMF (10 mL) to 100 °C for 5 h. Once cool, CH_2Cl_2 was added followed by washing with aqueous NH_4Cl , drying with Na_2SO_4 , and removal of all solvent at reduced pressure. Radial SiO_2 chromatography (SiO_2 , 1% Et_2O –petroleum ether) resulted in 22 mg (19%) of pure **2-TBS**: 1H NMR (CD_2Cl_2) δ 9.67 (d, 1H, $J = 16$ Hz), 9.59 (d, 2H, $J = 4.7$ Hz), 8.78 (d, 2H, $J = 4.6$ Hz), 8.63 (s, 4H), 7.85 (d, 2H, $J = 8.7$ Hz), 7.46 (d, 2H, $J = 8.1$ Hz), 7.39 (d, 1H, $J = 16$ Hz), 7.30 (s, 4H), 7.28 (s, 2H), 2.63 (s, 6H), 2.61 (s, 3H), 1.85 (bs, 18H), 1.22 (s, 9H), 1.00 (s, 9H), 0.02 (bs, 6H); ^{13}C NMR (CD_2Cl_2) δ 151.9, 150.5, 150.3, 150.1, 142.6, 139.8, 139.6, 138.1, 135.5, 131.5, 131.0, 129.3, 128.2, 126.4, 126.3, 119.5, 119.1, 117.8, 61.8, 26.7, 26.6, 22.0, 21.9, 21.8, 18.5, -4.2 ; UV–vis ($CHCl_3$) λ_{max} (log ϵ) 608 (4.13), 563 (4.28), 521 (3.86), 434 (5.44), 311 (4.44); IR (film) ν_{max} 3099, 2957, 2927, 2856, 2733, 1609, 1498, 1477, 1460 cm^{-1} ; MS–FAB $C_{65}H_{71}N_5O-SiZn$ calcd exact mass 1029.4719, obsd 1029.4697.

Zinc(II) 5-[4-[*N*-*tert*-butyl-*N*-(*tert*-butyldimethylsiloxy)-amino]phenylethynyl]-10,15,20-trimesitylporphyrin (3-TBS). A flask containing **6-TBS** (132 mg, 0.433 mmol), **20** (131 mg, 0.153 mmol), THF (6 mL), and triethylamine (1 mL) was sparged with argon for 30 min. $Pd(PPh_3)_4$ (27 mg, 0.023 mmol) and CuI (9 mg, 0.046 mmol) were added quickly with argon purging succeeded by stirring for 20 h. The solvent was removed in vacuo, and the residue was purified by flash chromatography (SiO_2 , 1% Et_2O –petroleum ether): 157 mg; 99%; 1H NMR ($CDCl_3$) δ 9.81 (d, 2H, $J = 4.7$ Hz), 8.85 (d, 2H,

$J = 4.7$ Hz), 8.67 (s, 4H), 7.95 (d, 2H, $J = 8.6$ Hz), 7.48 (d, 2H, $J = 7.8$ Hz), 7.32 (s, 4H), 7.29 (s, 2H), 2.67 (s, 6H), 2.64 (s, 3H), 1.89 (bs, 18H), 1.24 (s, 9H), 1.01 (s, 9H), 0.03 (bs, 6H); ^{13}C NMR ($CDCl_3$) δ 152.3, 151.8, 150.4, 150.1, 150.0, 149.6, 139.4, 139.0, 137.7, 131.6, 131.5, 131.4, 131.2, 130.9, 127.9, 125.6, 120.6, 120.4, 120.0, 100.0, 96.5, 92.3, 61.6, 26.5, 26.4, 21.9, 21.8, 21.7, 18.3, -4.3 ; UV–vis ($CHCl_3$) λ_{max} (log ϵ) 623 (4.35), 615 (4.34), 571 (4.22), 535 (3.65), 444 (5.59), 313 (4.37); IR (film) ν_{max} 2960, 2927, 2857, 1610, 1500, 1450 cm^{-1} . Anal. Calcd for $C_{65}H_{69}N_5O-SiZn$: C, 75.81; H, 6.75. Found: C, 76.02; H, 7.01.

1-[*N*-*tert*-butyl-*N*-(*tert*-butyldimethylsiloxy)amino]-4-ethynylbenzene (5-TBS). A 50 mL Schlenk flask containing methyltriphenylphosphonium bromide (1.58 g, 4.42 mmol) and THF (25 mL) was cooled in an ice bath. *n*-Butyllithium (2.25 M in pentane, 1.96 mL, 4.41 mmol) was added slowly via syringe. After being stirred for 3 h, the mixture was cooled to -78 °C and a solution of **10** (1.30 g, 4.24 mmol, in 5 mL THF) was added. Once stirred overnight, petroleum ether was added and the resulting mixture was washed twice with saturated aqueous NaCl. The organic mixture was dried (Na_2SO_4) and concentrated under reduced pressure. **5-TBS** (0.969 g, 75%) was isolated by flash chromatography (SiO_2 , petroleum ether): 1H NMR ($CDCl_3$) δ 7.27 (d, 2H), 7.19 (d, 2H, $J = 8.1$ Hz), 6.68 (dd, 1H, $J = 17.6$ Hz, 11.0 Hz), 5.69 (d, 1H, $J = 17.8$ Hz), 5.17 (d, 1H, $J = 10.8$ Hz), 1.09 (s, 9H), 0.90 (s, 9H), -0.13 (bs, 6H); ^{13}C NMR ($CDCl_3$) δ 136.8, 134.4, 126.6, 125.6, 125.4, 112.9, 48.84, 26.35, 18.21, -4.40 ; IR (film) ν_{max} 3088, 3037, 2960, 2929, 2890, 2857, 1631, 1605, 1504, 1472, 1462 cm^{-1} . Anal. Calcd for $C_{18}H_{31}NOSi$: C, 70.76; H, 10.23. Found: C, 70.49; H, 10.27.

1-[*N*-*tert*-butyl-*N*-(*tert*-butyldimethylsiloxy)amino]-4-ethynylbenzene (6-TBS). A flask containing **11-TBS** (0.844 g, 2.35 mmol), (trimethylsilyl)acetylene (0.67 mL, 0.463 g, 4.70 mmol), and triethylamine (10 mL) was sparged with argon for 30 min. $Pd(PPh_3)_4$ (0.277 g, 0.24 mmol) was added quickly with argon purging succeeded by heating to reflux for 5 h. Once cool, the mixture was filtered through SiO_2 with petroleum ether rinsing. The solvent was removed in vacuo, and the residue was purified by flash chromatography (SiO_2 , petroleum ether). The resulting trimethylsilyl-protected **6-TBS** (0.612 g, 1.63 mmol) was stirred with K_2CO_3 (0.478 g, 3.46 mmol) in THF–MeOH (3:1, 12 mL) for 16 h. Petroleum ether was added, and the solution was washed with saturated aqueous NaCl followed by drying (Na_2SO_4) and concentration under reduced pressure. The residue was subjected to reversed-phase medium-pressure liquid chromatography (LiChroprep RP-18, methanol) with UV (254 nm) isolating **6-TBS** (0.486 g, 68%): 1H NMR ($CDCl_3$) δ 7.36 (d, 2H, $J = 8.7$ Hz), 7.19 (d, 2H, $J = 8.1$ Hz), 3.03 (s, 1H), 1.08 (s, 9H), 0.90 (s, 9H), -0.13 (bs, 6H); ^{13}C NMR ($CDCl_3$) δ 151.9, 131.3, 125.0, 118.1, 83.9, 76.4, 61.2, 18.0, -4.7 ; IR (film) ν_{max} 3318, 3090, 3039, 2956, 2930, 2884, 2856, 2110, 1602, 1494, 1471 cm^{-1} . Anal. Calcd for $C_{18}H_{29}NOSi$: C, 71.23; H, 9.63. Found: C, 71.41; H, 9.52.

1-[*N*-*tert*-butyl-*N*-(*tert*-butyldimethylsiloxy)amino]-4-phenylbenzene (7-TBS). A flask containing bromobenzene (0.026 mL, 0.251 mmol) and $Pd(PPh_3)_4$ (0.0087 g, 0.0075 mmol) in THF (10 mL) was stirred while sparging with argon for 20 min. Compound **12** (0.100 g, 0.279 mmol) and Na_2CO_3 (2 M, 0.28 mL) were added quickly with argon purging, and the mixture was refluxed for 12 h. Once cool, the mixture was filtered through a glass filter with petroleum ether rinsing to remove inorganic solids. The resulting mixture was washed twice with saturated aqueous NaCl followed by drying with $MgSO_4$. The solvent was removed under reduced pressure. The remaining oil was purified by radial chromatography with pentane to give **7-TBS** (0.030 g, 30%): 1H NMR (CD_2Cl_2) δ 7.62 (d, 2H), 7.50 (d, 2H), 7.43 (t, 3H), 7.33 (d, 2H), 1.14 (s, 9H), 0.94 (s, 9H), -0.07 (bs, 6H); ^{13}C NMR (CD_2Cl_2) δ 151.0, 141.2, 137.7, 129.1, 127.3, 127.1, 126.1, 126.0, 61.3, 26.4, 26.3, 18.3, -4.5 ; IR (film) ν_{max} 3032, 2958, 2930, 2857, 1605, 1485, 1472, 1462 cm^{-1} ; MS m/z 355 (M^+ , 17), 299 (38), 242 (62), 224 (100), 210 (25), 167 (87).

2'-Methyl-4-[*N*-*tert*-butyl-*N*-(*tert*-butyldimethylsiloxy)-amino]biphenyl (8-TBS). A 50 mL flask containing 2-bro-

motoluene (0.067 mL, 0.558 mmol) and Pd(PPh₃)₄ (0.0193 g, 0.0167 mmol) in THF (20 mL) was stirred while sparging with argon for 5 min. Compound **12** (0.2 g, 0.558 mmol) and aqueous Na₂CO₃ (2M, 0.56 mL) were added quickly with argon purging and refluxed for 2 days. Once cool, the solvent was removed by rotary evaporation, and the mixture was dissolved in petroleum ether, filtered through a plug of Celite, and concentrated under reduced pressure. The resultant oil was purified by chromatography on a Chromatotron, eluting with pentane to give **8-TBS** (0.0507 g, 25%): ¹H NMR (CD₂Cl₂) δ 7.28–7.14 (m, 8H), 2.23 (s, 3H), 1.14 (s, 9H), 0.92 (s, 9H), –0.09 (bs, 6H); ¹³C NMR (CD₂Cl₂) δ 150.0, 142.1, 138.6, 130.5, 130.01, 128.2, 125.9, 125.1, 61.1, 26.4, 20.7, 18.2, –4.5. Anal. Calcd for C₂₃H₃₆NOSi: C, 74.53; H, 9.79. Found: C, 74.57; H, 9.52.

2',4',6'-Trimethyl-4-[N-tert-butyl-N-(tert-butyldimethylsilyloxy)amino]biphenyl (9-TBS). A 25 mL flask containing 2-bromomesitylene (0.086 mL, 0.558 mmol), Pd(PPh₃)₄ (0.0193 g, 0.0167 mmol), compound **12** (0.2 g, 0.558 mmol), anhydrous DMF (4 mL), and distilled toluene (2 mL) was stirred while sparging with argon for 10 min. K₃PO₄ (0.1778 g, 0.8376 mmol) was added quickly with argon purging and heated for 2 days. Once cool, the solvent was removed by bulb-to-bulb vacuum distillation and the residue dissolved in petroleum ether, filtered through a plug of Celite column, and evaporated under reduced pressure. The resultant oil was purified by chromatography on a Chromatotron, eluting with pentane to give, after evaporation of solvent, a white solid, **9-TBS** (0.1229 g, 55%): ¹H NMR (CD₂Cl₂) δ 7.29 (d, 2H), 6.96 (d, 2H), 6.91 (s, 2H), 2.29 (s, 3H), 1.97 (s, 6H), 1.14 (s, 9H), 0.92 (s, 9H), –0.08 (bs, 6H); ¹³C NMR (CD₂Cl₂) δ 150.0, 137.9, 136.6, 136.3, 128.5, 128.2, 125.8, 61.0, 26.3, 21.1, 20.7, 18.3, –4.6. Anal. Calcd for C₂₅H₄₀NOSi: C, 75.31; H, 10.11. Found: C, 75.41; H, 10.05.

4-[N-tert-butyl-N-(tert-butyldimethylsilyloxy)amino]phenylpinacol Boronate (12). In a 100 mL Schlenk flask, **11-TBS** (0.991 g, 2.76 mmol) was dissolved in 15 mL of distilled THF and cooled to –78 °C. *tert*-Butyllithium (3.72 mL, 5.58 mmol) was slowly added over 40 min. The reaction mixture was stirred for 1 h at –78 °C. Trimethyl borate (1.10 mL, 9.67 mmol) was added and stirred overnight. Pinacol (0.980 g, 8.29 mmol) was added and stirred for 10 h. The reaction mixture was washed with saturated NaCl twice. The organic layer was dried over MgSO₄. The solvent was removed under reduced pressure. The remaining yellow oil was purified by radial chromatography (1% Et₂O–petroleum ether) and then recrystallized from methanol to give **12** (0.721 g, 64%) as a white solid: ¹H NMR (CDCl₃) δ 7.67 (d, 2H), 7.23 (d, 2H), 1.34 (s, 12H), 1.08 (s, 9H), 0.90 (s, 9H), –0.14 (s, 6H); ¹³C NMR (CDCl₃) δ 154.1, 133.9, 124.4, 83.6, 61.1, 26.2, 26.1, 25.0, 18.0, –4.6; IR (film) ν_{max} 2979, 2930, 2858, 1605, 1564, 1472, 1462, 1360 cm^{–1}. Anal. Calcd for C₂₂H₄₀NBO₃Si: C, 65.17; H, 9.94. Found: C, 65.07; H, 9.86.

5,10,15-Trimesitylporphyrin. Dipyrromethane (1.33 g, 9.0 mmol), *meso*-mesityldipyrromethane (2.38 g, 9.0 mmol), and mesitaldehyde (2.67 g, 18.0 mmol) were dissolved in 1800 mL of chloroform. Boron trifluoride etherate (0.66 mL, 5.4 mmol) was added, and the mixture was stirred for 30 min. TEA (6.3 mL, 45 mmol) and DDQ (6.13 g, 27 mmol) were then added, followed by stirring for 1 h. The mixture was poured over silica (120 mm × 8 in) and eluted with CH₂Cl₂ until all porphyrins eluted. The porphyrins were then separated by gravity elution, silica chromatography (petroleum ether to 1% Et₂O–petroleum ether), and alumina chromatography (petroleum ether to 3% Et₂O–petroleum ether). **19** (0.716 g, 12%): ¹H NMR (CDCl₃) δ 10.23 (s, 1H), 9.39 (d, 2H, *J* = 4.6 Hz), 8.99 (d, 2H, *J* = 4.6 Hz), 8.86 (s, 4H), 7.46 (s, 4H), 7.43 (s, 2H), 2.78 (s, 6H), 2.76 (s, 3H), 2.03 (bs, 18H), –2.60 (bs, 2H); ¹³C NMR (CDCl₃) δ 146.3 (broad), 139.8, 138.9, 138.3, 138.0, 131.7, 130.8, 130.4, 130.3, 128.1, 128.0, 118.4, 117.7, 104.3, 22.0, 21.7. Anal. Calcd for C₄₇H₄₄N₄: C, 84.90; H, 6.67. Found: C, 85.06; H, 6.77.

5-Iodo-10,15,20-trimesitylporphyrin. 5,10,15-Trimesitylporphyrin (0.421 g, 0.633 mmol), chloroform (10 mL), bis-

(trifluoroacetoxy)iodobenzene (0.201 g, 0.467 mmol), and iodine (0.096 g, 0.380 mmol) were stirred for 1 h. The mixture was poured into CH₂Cl₂, washed with aqueous Na₂S₂O₃, and dried with MgSO₄. The residue after solvent evaporation was chromatographed on alumina (1–3% Et₂O–petroleum ether). **20** (0.364 g, 73%): ¹H NMR (CDCl₃) δ 9.61 (d, 2H, *J* = 4.9 Hz), 8.72 (d, 2H, *J* = 4.7 Hz), 8.60 (s, 4H), 7.30 (s, 4H), 7.27 (s, 2H), 2.65 (s, 6H), 2.62 (s, 3H), 1.86 (bs, 18H), –2.47 (bs, 2H); ¹³C NMR (CD₂Cl₂) δ 147.2 (broad), 139.9, 139.8, 138.6, 138.5, 138.2, 137.4, 132.1, 131.3, 128.4, 119.7, 119.5, 77.80, 21.9, 21.8; IR (film) ν_{max} 3057, 2957, 2857, 2160, 2108, 1602, 1480 cm^{–1}. Anal. Calcd for C₄₇H₄₃N₄I: C, 71.38; H, 5.48. Found: C, 71.36; H, 5.87.

Zinc(II) 5-Iodo-10,15,20-trimesitylporphyrin (19). A mixture of 5-iodo-10,15,20-trimesitylporphyrin (0.363 g, 0.459 mmol), chloroform (10 mL), and zinc(II) acetate (0.202, 0.918) was heated to a gentle reflux for 2 h. The mixture was poured into CH₂Cl₂, washed with aqueous NaHCO₃, and dried with MgSO₄. The residue after solvent evaporation was chromatographed on alumina (1–3% Et₂O–petroleum ether). **21** (0.351 g, 89%): ¹H NMR (CDCl₃) δ 9.72 (d, 2H, *J* = 4.6 Hz), 8.80 (d, 2H, *J* = 4.6 Hz), 8.68 (bs, 4H), 7.30 (s, 4H), 7.28 (s, 2H), 2.65 (s, 6H), 2.63 (s, 3H), 1.86 (bs, 18H); ¹³C NMR (CDCl₃) δ 152.1, 151.0, 150.5, 150.4, 139.5, 139.0, 138.2, 137.8, 132.3, 131.8, 131.6, 127.9, 119.9, 80.0, 22.0, 21.9, 21.7; LD-MS C₄₇H₄₁N₄Izncalcd mass 852.2; obsd 852.3.

General Procedure for TBS-Deprotection and Subsequent Oxidation of Hydroxylamine Porphyrins. The TBS-protected metalloporphyrin (>0.01 mmol) was dissolved in 1 mL of THF and subsequently treated with 1 equiv of Bu₄NF (1 M in THF). Upon completion of the reaction (as detected by TLC, usually <3 h), the solution was washed with aqueous NH₄Cl that had been sparged with argon for 30 min, dried with Na₂SO₄, and concentrated with a stream of argon providing the hydroxylamine. EPR samples were prepared in a glovebox by dissolution of the hydroxylamine in an appropriate amount of toluene (0.2 mM) and transfer to a quartz tube containing an excess of PbO₂. Oxidation for UV–vis and IR samples was accomplished by stirring a THF solution of the hydroxylamine (as prepared above) with 20 equiv of PbO₂ for 1–3 h (completion detected by TLC), evaporating the THF with a stream of argon and purifying with a small SiO₂ column.

1: IR (film) ν_{max} 3098, 2961, 2925, 2734, 1456, 1342, 1272, 1000, 802 cm^{–1}; UV–vis (CHCl₃) λ_{max} (log ε) 580 (3.26), 541 (4.15), 502 (3.50), 417 (5.38), 306 (4.21).

2: IR (film) ν_{max} 3110, 2958, 2922, 2854, 2732, 1454, 1205, 997, 797 cm^{–1}; UV–vis (CHCl₃) λ_{max} (log ε) 614 (4.31), 562 (4.35), 433 (5.46), 311 (4.55).

3: IR (film) ν_{max} 3112, 2959, 2923, 2954, 2733, 2187, 1205, 997, 798 cm^{–1}; UV–vis (CHCl₃) λ_{max} (log ε) 621 (4.64), 566 (4.43), 526 (4.01), 468 (4.95), 441 (5.46), 433 (5.46), 317 (4.57).

Acknowledgment. This work is supported by the National Science Foundation (CHE-9501085) under the CAREER Program and the Research Corporation (CS0127) under the Cottrell Scholars Program. Mass spectra were obtained at the Mass Spectrometry Laboratory for Biotechnology. Partial funding for the Facility was obtained from the North Carolina Biotechnology Center and the National Science Foundation. The MALDI-TOF mass spectrometer was funded in part by the North Carolina Biotechnology Center. The GC-MS instrument was purchased with funds from Hewlett-Packard through their Grants for Universities Program.

Supporting Information Available: Spectral data (51 pages). This material is contained in libraries on microfiche, immediately follows this article in the microfilm version of the journal, and can be ordered from the ACS; see any current masthead page for ordering information.

JO971736Q